Faculty and Researchers | Faculty and Researchers' Publications

2010

Friction stir processing (FSP): refining microstructures and improving properties

McNelley, T.R.

Friction stir processing (FSP): refining microstructures and improving properties

T.R. McNelley*

Abstract   FSP is reviewed as an allied technology of friction stir welding (FSW) and additional considerations such as processing pattern and step over distance are introduced. The application of FSP to continuously cast AA5083 material in the as-cast condition is described and the extent of grain refinement and homogenization of microstructure is documented. The FSP-induced superplastic response of this material is compared to the response of conventionally processed AA5083 and the improved ductility of the FSP material is related to grain refinement and microstructure homogenization.

Keywords   Friction stir processing; Grain refinement; Homogenization; Mechanical properties; Superplasticity.

Procesado por fricción batida (FSP): afino de la microestructura y mejora de propiedades

Resumen   Se revisa el procesado por fricción batida (FSP) como un aliado tecnológico de la soldadura por fricción batida (FSW) y se introducen consideraciones adicionales tales como el patrón de procesado y el paso en función de la distancia. Se describe la aplicación de FSP al material AA5083 por colada continua en la condición de colada y se documenta el grado de afino de grano y homogeneización de la microestructura. La respuesta de superplasticidad inducida por FSP se compara con la respuesta de la aleación AA5083 procesada convencionalmente y la mejora de ductilidad del material FSP se relaciona con el afino de grano y la homogeneización de la microestructura.

Palabras clave   Procesado por fricción batida; Afino de grano; Homogeneización; Propiedades mecánicas; Superplasticidad.

1. INTRODUCTION

Friction stir processing (FSP) is a solid-state technique involving the use of a non-consumable rotating tool to refine and homogenize microstructures in metallic components[1 and 2]. It is among the allied processes of friction stir welding (FSW), a solid-state joining method originally developed by The Welding Institute[3]. All FS technologies rely on a severe but localized thermomechanical cycle induced by tool action on a deformable metallic material.

The initial motivation for the development of FSW was the desire to circumvent the problem of solidification cracking that is often encountered in fusion welding in many high-strength aluminum alloys[3]. FSW has now been applied successfully to a wide range of Al, Mg, Cu, Fe and Ti alloys. The basic concept of FSW is straightforward. The parts to be joined are abutted and fixed against a rigid restraint that serves as an anvil, as illustrated in figure 1 a). A cylindrical, wear-resistant tool consisting of a smaller diameter pin with a concentric, larger-diameter shoulder is rotated while the pin is forced into the surfaces of the parts at a point along the abutment line; this is indicated in figure 1 b). A combination of frictional and adiabatic heating results in the formation of a plasticized column of metal and a localized 'stirring' action involving deformation and motion of material around the tool pin as it penetrates (Fig. 1 c)). When the shoulder comes in contact with the part surfaces the tool is traversed along the abutment line and the flow of material about the tool pin leads to coalescence across the faying surfaces and the formation of a weld, as

* Department of Mechanical and Aerospace Engineering, Naval Postgraduate School, 700 Dyer Road, Monterey, California 93943-5146 · USA. Email: *tmcnelley@nps.edu.*
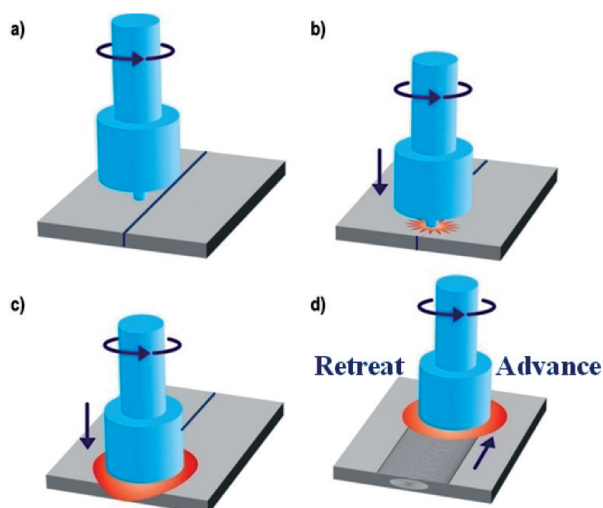
Figure 1. A schematic of FSW/P, showing the rotating, non-consumable tool in (a), frictional heating upon plunging into the work piece in (b), frictional and adiabatic heating in (c) and traversing of the tool to weld/process the work piece in (d).

Figura 1. Esquema de FSW/P mostrando la herramienta de rotación permanente en a), calentamiento por fricción después de penetrar en el material en b), calentamiento de fricción y adiabático en c) y desplazamiento de la herramienta para procesar/soldar el objeto de trabajo (d).

suggested in figure 1 d). Single-pass, single-sided welds are readily produced by FSW wherein the pin length is slightly less than the thickness of the joint so that the pin does not come in contact with the anvil. The tool shoulder helps to control tool penetration and is necessary to constrain upward metal flow; it also forges the weld nugget. Many tool design features have been evaluated and critical process parameters include tool rpm and traversing rates. Aluminum materials of thicknesses varying from <1mm to >25mm have been joined by FSW and many variations on the basic concept of FSW have been reported in recent years[2].

As one of these variations, FSP involves a single work piece and traversing of the tool following a predetermined pattern over the work piece surface of to process a volume of material defined by the pin tool profile and the processing pattern[4 and 5]. The full thickness of the work piece may be processed as in FSW. However, in other applications the work piece may be thicker that the pin length so that only a surface layer is subjected to the FSP thermomechanical cycle. The depth of this layer is limited mainly by tool design, available power and capability of reacting and

controlling the downward, or plunge, force needed to accomplish FSP. This FS technology has been conducted on cast as well as wrought metals including alloys of Al and Mg as well as higher melting alloys of Cu, Fe and Ti [4]. When applied to an as-cast metal such as NiAl bronze, the FSP thermomechanical cycle converts the as-cast microstructure to a wrought condition in the absence of macroscopic shape change. Phase transformations induced by FSP result in highly refined grains as well as homogenization within the stir zone. In turn, yield and ultimate strengths are both raised while ductility is also increased within the volume of processed material, so that FSP produces a surface hardening effect in as-cast NiAl bronze[5-9]. In this paper further background on FSP will be summarized and the potential for grain refinement sufficient to support extensive superplasticity in a continuously cast AA5083 material initially in the as-cast condition will be outlined.

2. FSP PROCEDURES

The tool traversing pattern and the 'step over' distance between adjacent passes during multi-pass processing are important additional process parameters in FSP. These are illustrated in figure 2. The traversing pattern may involve only a single linear or curvilinear processing pass as illustrated in figure 2 a). A larger volume of material may be subjected to the FSP thermomechanical cycle by a series of linear traverses offset from one another by stepping over by a pre-selected distance as indicated in figure 2 b). Due to tool rotation the deformation field about the tool pin is not symmetric about the axis of tool advance and so there is variation in microstructure from the advancing side (tool surface speed and traversing speed add; figure 1 d) to the retreating side (tool surface speed and traversing speed subtract; figure 1 d). Microstructure gradients are typically more pronounced on the advancing side than on the retreating side. A series of parallel traverses as suggested in figure 2 b) result in successive replacement of the advancing interfaces with retreating interfaces in the processed volume of material. In contrast, a raster pattern as shown in figure 2 c) results in a pattern of advancing/advancing and retreating/retreating interfaces in a direction transverse to the local direction of tool advance. Such a pattern may leave long-range gradients in microstructure in the stir zone and lead to strain localization with attendant low transverse ductility. The use of a spiral pattern such as that illustrated in figure 2 d) results in the replacement of the advancing interface with a retreating interface on
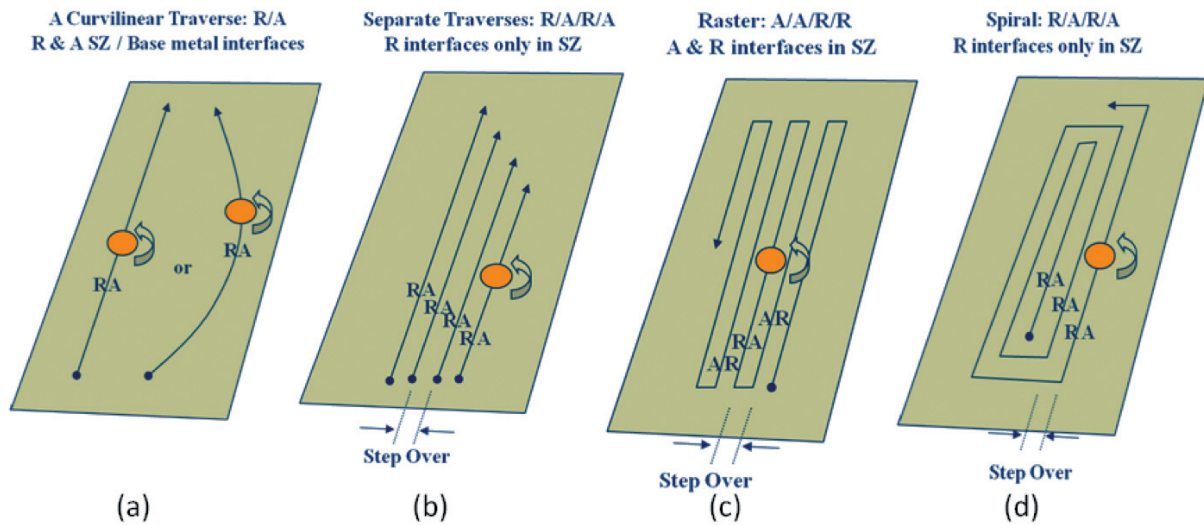
Figure 2. Traversing patterns for FSP: a single linear or curvilinear pass is shown in (a), multi-pass FSP may involve parallel passes offset by a step over distance as in (b), or a raster pattern, (c), or a spiral pattern, (d).

Figura 2. Patrones de recorrido de FSP: se muestra una sola línea o una curvilínea en a), pasadas múltiples por FSP pueden involucrar pasadas paralelas terminadas por un escalón, como en b), o un patrón de muestreo, c), o un patrón en espiral, d).

successive passes and thus may mitigate gradients in stir zone microstructure.

The step over distance is typically based on the pin diameter in order to assure overlap of stir zones on successive passes in multi-pass processing. The stir zone is generally wider at the work piece surface due to the effect of the tool shoulder, and an excessive step over distance may result in incomplete overlap in lower regions of the stir zone on successive passes. Again, microstructure gradients within the stir zone may result in strain localization and reduced ductility. Using a step over distance that is ≈½ of the pin diameter at the mid-length of the pin generally eliminates such microstructure gradients.

3. FSP OF CONTINUOUSLY CAST AA5083 IN THE AS-CAST CONDITION

The processes of superplastic forming (SPF) and quick plastic forming (QPF) of AA5083 are of interest for transportation applications[10]. Material produced by conventional direct-chill casting may be processed by hot working and subsequent cold working so that recrystallization upon heating of 1-2 mm thick sheet material to the forming temperature of 450 °C gives a grain size of ≈7 µm. Such a grain size supports good tensile and biaxial ductility during SPF and QPF [11-15]. The introduction of continuously cast (CC) AA5083 into this process would reduce costs[10]. However, as-cast CC slab is typically only ≈15 mm in thickness and thus cannot be strained sufficiently during hot and cold working to homogenize and refine microstructure as well as produce sheet material. Thus, ductility of the CC AA5083 is marginal SPF and QPF applications[11, 13 and 14]. This investigation was conducted to assess the extent of stir zone grain refinement attainable by FSP of CC AA5083 and to determine whether the resulting microstructures would improve the superplastic response of this material.

Details of the CC AA5083 alloy of this investigation have been given previously[11 and 13]. The material was provided by Commonwealth Aluminum, Inc., in the form of a 15 mm thick slab in the as-cast condition. The composition of this material falls within the limits of AA5083 and is summarized in table 1. A plate for FSP was sectioned from as-received material and surfaces were machined prior to processing. FSP was conducted on these plates using tools fabricated in H13 tool steel and heat treated to HRC52. The tool pins were 3 mm in diameter. One tool had a 5 mm pin length while a second had a pin 3 mm in length. Both tools had a shoulder diameter of 10 mm. The tool shown in figure 3 a) had a 3 mm pin length; both tool designs included a thread feature. Results for two experimental runs will be presented here. The first

Table I. Composition data for the continuously cast AA5083 material

Tabla I. Composición del material AA5083 por colada continua

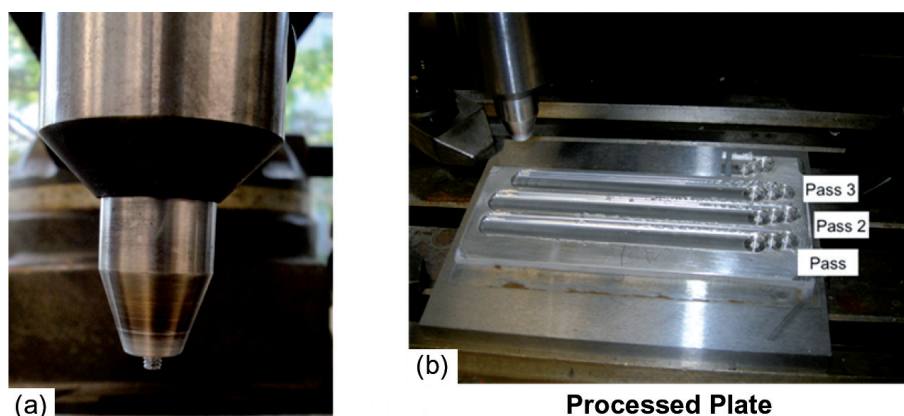| Element	Mg	Mn	Si	Fe	Cr	Cu	Zr
Wt. Pct	4.616	0.735	0.102	0.191	0.249	0.025	0.001

Figure 3. The FSP tool is shown in (a) and a plate processed by multi-pass FSP involving parallel, offset passes in (b).

Figura 3. Se muestra la herramienta en (a) y una chapa procesada por múltiples pasadas de FSP por medio de pasadas paralelas con escalones en (b).

run involved three overlapping FSP traverses as illustrated in figure 2 b), with a tool rotation rate of 350 rpm and traversing rate of 101.6 mm min⁻¹ using the longer pin tool. The second involved three successive overlapping FSP traverses with a tool rotation rate of 800 rpm and a traversing rate of 76.2 mm min⁻¹ using the shorter pin tool. In both cases the step over distance was 2 mm. The as-processed plate for the latter rpm and traversing rate combination is shown in figure 3 b).

Details of metallographic preparation have also been given in previous reports[15]. For optical microscopy, conventional grinding and polishing through 0.5 μm diamond abrasive was followed by etching in a 10 % phosphoric acid –90 % water solution at 50 °C. Imaging was accomplished using a Nikon Epiphot 200 inverted microscope. Scanning electron microscopy (SEM) and orientation imaging microscopy (OIM) required an additional electropolishing step utilizing a solution of 80 % ethanol, 6 % perchloric acid and 14 % water and a voltage of 15 VDC. Backscatter imaging was utilized in a Zeiss Neon40 Field Emission FE-SEM. OIM analysis employed an EDAX-TSL system equipped with a Hikari camera. Sample thinning for scanning transmission electron microscopy (STEM) imaging in the scanning electron microscope was carried out using a focused ion beam (FIB) attachment on the FE-SEM.

4. MICROSTRUCTURE REFINEMENT AND SUPERPLASTICITY

Transverse sections through the stir zones of materials processed during runs 1 and 2 are shown in figure 4 a) and b), respectively. Examination of figure 4 a) reveals a tunnel defect on the lower advancing side of the stir zone, likely reflecting insufficient heating and deformation to move material around the tool pin. In contrast, no defects are visible in the transverse section from run 2 for material processed at a higher rpm. However, the tool penetration was likely greater in this case and this is evident in the apparent depression below the surrounding surface at the top of this transverse section.

The homogenization as well as refinement of micrsostructure that may be attained during FSP of this material is illustrated in figure 5. These images were acquired from material processed during run 1 (Fig. 4 a)). An optical micrograph from the unaffected
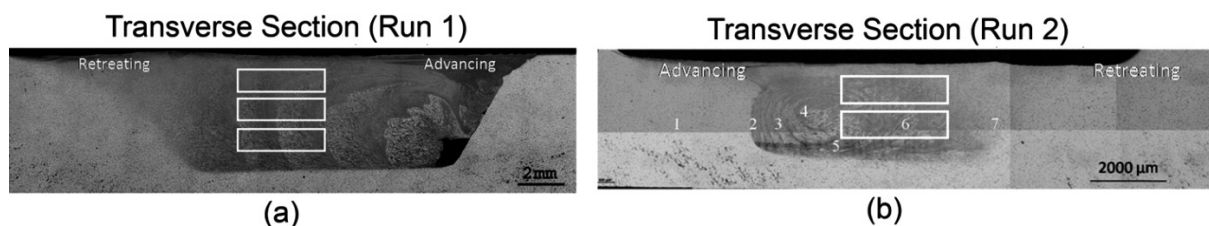
Figure 4. Transverse sections showing material processed at 350 rpm and 101.6 mm min^{-1} in (a), and at 800 rpm and 76.2 mm min^{-1} in (b). A tunnel defect is apparent at the lower right of the stir zone in (a). The rectangular boxes indicate approximate locations of the tensile gage sections.

Figura 4. Cortes transversales mostrando el material procesado a 350 rpm y 101,6 mm min^{-1} en (a), y a 800 rpm y 76,2 mm min^{-1} en b). Se observa un defecto de túnel en la parte inferior derecha de la zona de batida en (a). Los rectángulos indican aproximadamente los lugares de las secciones de la longitud de trabajo en tracción.
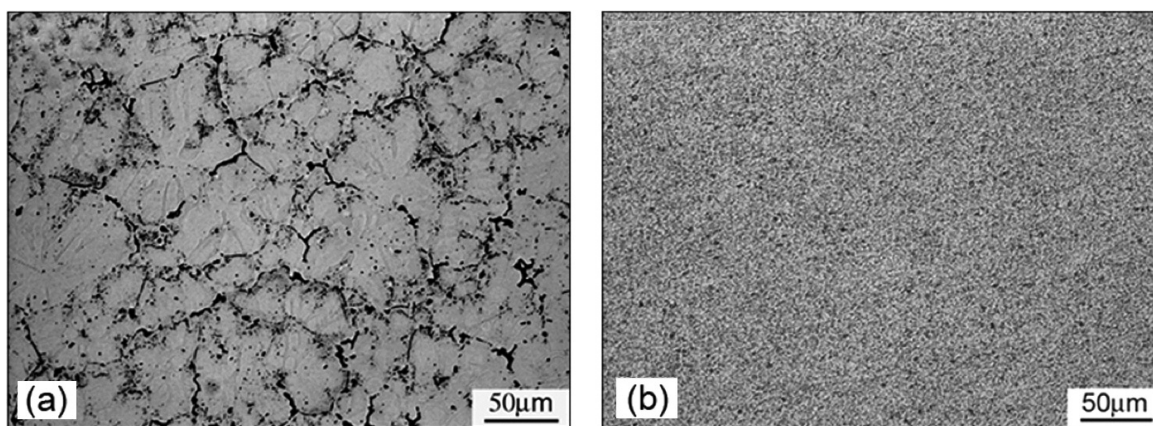

Figure 5. The as-cast base material is shown in (a) and homogenization and refinement due to FSP during run 1 are apparent in (b). The as-cast base material microstructure comprises primary α (light etching) and a eutectic which is mainly β (Al$_8$Mg$_5$).

Figura 5. Los materiales base de colada se muestran en (a) y la homogeneización y el afino por FSP durante una pasada se muestra en (b). La microestructura del material base de colada de un primario (ataque claro) y un eutéctico que es, principalmente, Al$_8$Mg$_5$.

base metal distant from the stir zone is presented in figure 5 a). The as-cast grain size in the primary α constituent appears to be equiaxed and ≈50 μm in size. The dark-etching constituent is a eutectic comprising mainly the β phase (Al$_8$Mg$_5$) and dispersed particles of the MnAl$_6$ phase are also apparent. Careful examination of the primary constituent in this micrograph reveals contrast variation suggesting cellular or dendritic growth during solidification of this material during continuous casting. Extensive refinement and homogenization is apparent in figure 5 b), which is a micrograph from the stir zone in figure 4 a). The grain size in the α phase cannot be discerned at the magnification in this image and the primary

α / eutectic features in the as-cast condition are no longer distinguishable in this image. However, it is apparent that both the eutectic   has been refined in size and re-distributed in the microstructure and the MnAl$_6$ particles have also be re-distributed. It is also noteworthy that no cavities or other features that might be associated with cracking of particles are apparent in this image.

A highly refined stir zone grain size is apparent in the backscatter electron image of figure 6 a). The β phase particles (dark in appearance) appear to be sub-micron in size and are often distributed on the grain boundaries of the α phase grains. In some locations, the β particles form a necklace-like structure on these grains. In contrast, the MnAl$_6$ particles (light in
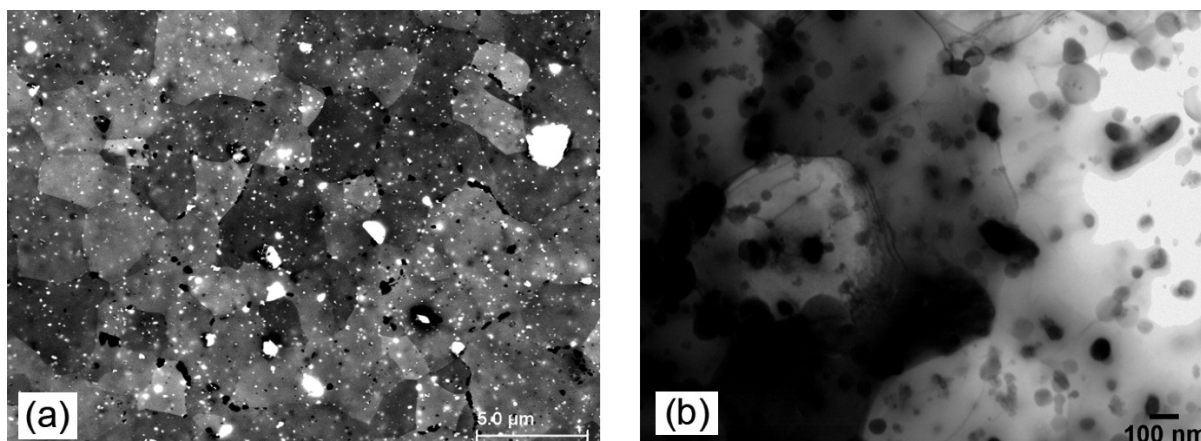
Figure 6. A backscatter electron image showing refined α grains and dispersed β (Al_8Mg_5) particles (dark contrast) and $MnAl_6$ particles (light contrast) is presented in (a). An STEM image of this material in (b) shows that FSP produces dispersed particles 10-30 nm in size dispersed throughout the refined grain structure.

Figura 6. Se presenta una imagen de electrones retrodispersados mostrando el afino del grano α y partículas dispersas β (Al_8Mg_5) (contraste oscuro) y partículas $MnAl_6$ (contraste claro) en (a). Una imagen de STEM de este material en (b) muestra que FSP produce partículas dispersas de tamaño de 10-30 nm distribuidas en una estructura de grano afinada.

appearance) are more or less uniformly distributed throughout the matrix; most of these particles are sub-micron in size although several large (0.5-2.0 μm) particles may also be seen. The refined grains are also apparent in the STEM image in figure 6 b) and fringe patterns at some boundaries suggest that high-angle boundaries surround grains as fine as 300 nm in size. Finely dispersed particles 10-100 nm in size are distributed throughout this microstructure.

Grain sizes for both processing runs were obtained by use of OIM methods. The results of OIM analysis are presented in figure 7 a) for material processed during run 1 and for material processed during run 2 in figure 7 b). The mean linear intercept grain size in figure 7 a) for run 1 was determined to be ≈1.2 μm while that in figure 7 b) for run was ≈3.5 μm. Grain-to-grain misorientations include a population of low-angle (0-5° mistorientation) boundaries in an otherwise random distribution with a peak at 45° in both cases. The texture appears to be random as well in figure 7 a) while a weak B-type shear texture component appears to have formed in the material processed during run 2.

The results of the microstructure analysis indicate that highly refined grains as fine as 1 μm in size may be attained during FSP of the as-cast material. In contrast, grain sizes of 7-8 μm were reported for both direct-chill cast and continuously cast AA5083 materials after conventional hot and cold rolling prior to reheating and recrystallization during forming. Thus, a series of

tension tests were conducted on materials process during the FSP runs. Tensile samples were obtained by wire electro discharge machining (EDM) in order to assure that the gage sections were completely within the stir zones (Fig. 4). After lightly grinding to remove machining damage these samples were pulled to failure at various strain rates and a test temperature of 450 °C.

The results of these tests are presented in figure 8 a) as the flow stress at a strain of 0.1 as a function of strain rate, and in figure 8 b) as the corresponding data for ductility as a function of strain rate. The data for the FSP material are shown as the solid lines while data for conventionally rolled direct-chill (DC) cast material and continuously-cast (CC) material are shown by the dotted lines. The plots in figure 8 a) show that the grain size refinement reduces the flow stress dramatically. For example, at a strain rate of 2×10^{-2} s^{-1} the flow stress of the material processed as FSP run 1, denoted as FSP (Ex1) in figure 8, is lower by a factor of six when compared to the conventionally processed material. The flow-stress vs. strain rate response of superplastic materials is often characterized by the power law relationship $\sigma = K\dot{\varepsilon}^m$, where σ is the flow stress, K is a material constant, $\dot{\varepsilon}$ is the strain rate, and m is the strain rate sensitivity coefficient. Here, it is apparent that refining grain size also leads to an increase in the strain rate sensitivity $m \rightarrow 0.5$ and for the finest grain size material. Such an m-value is consistent with the ductility of 1,200 pct. at a strain rate of 10^{-1}s^{-1}, which
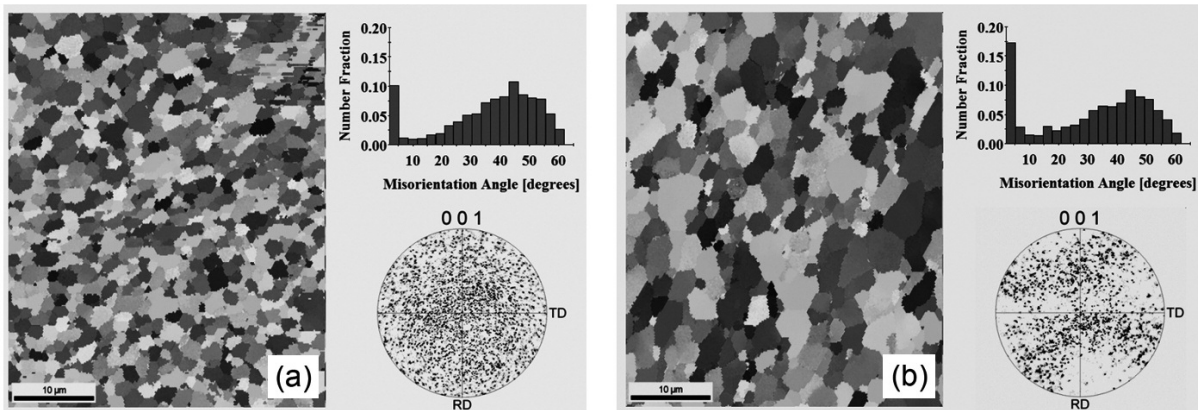
Figure 7. OIM data showing refinement to grains ≈1.2 μm in size during run 1 (a). Grains ≈3.5 μm in size were obtained during run 2 at a higher rpm and slower traversing rate. Random grain boundaries with a superimposed population of low-angle grain boundaries are evident in both materials and a weak B-type shear texture has been retained in run 2 material.

Figura 7. Datos de OIM mostrando afino de grano hasta tamaños ≈1,2 μm durante la primera pasada (a). Se obtuvieron granos de tamaño ≈3,5 μm en la segunda pasada a mayores revoluciones y menor velocidad de desplazamiento. Se observan en ambos materiales fronteras de grano al azar superpuestas a una población de fronteras de grano de bajo ángulo reteniéndose una débil textura de cizalla de tipo B en el material con dos pasadas.
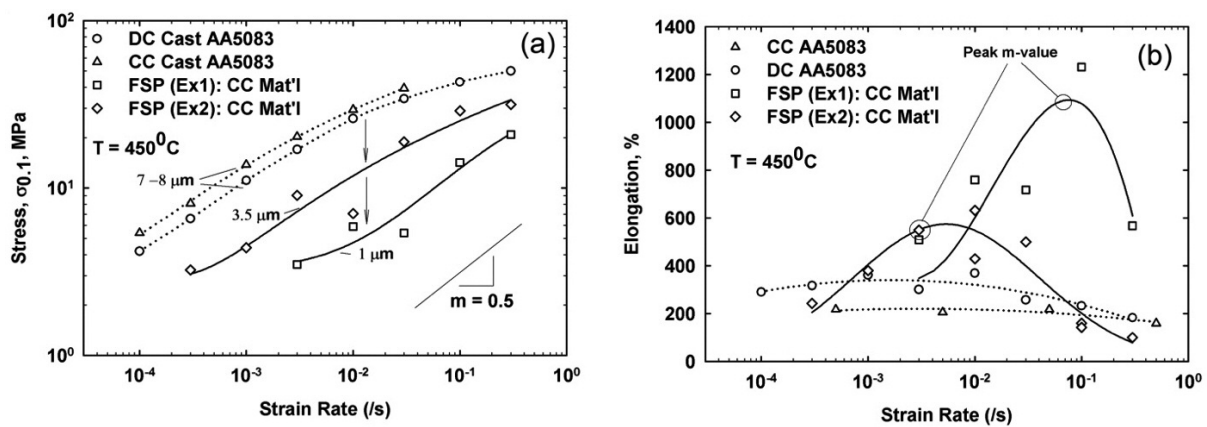

Figure 8. Mechanical property data for AA5083 material in the form of flow stress as a function of strain rate, (a), and ductility as a function of strain rate, (b), for continuously cast (CC) materials processed by FSP (solid lines) and materials processed by conventional hot and cold rolling after either direct-chill (DC) casting or continuous casting (CC) dotted lines.

Figura 8. Datos de propiedades mecánicas del material AA5083 en forma de tensión de fluencia en función de la velocidad de deformación, (a), y ductilidad en función de la velocidad de deformación, (b), para materiales de colada continua (CC) procesados por FSP, líneas continuas, y materiales procesados por laminado en frío y en caliente después de colada con enfriamiento rápido directo (DC) o colada continua (CC), líneas de puntos.

is the strain rate of the maximum for m. It is noteworthy that the flow stress at this strain rate of 10 pct/s is equal only to that of conventional material at a strain rate that is 100 times lower! The ductility

reported here for AA5083 material appears to be the highest superplastic ductility reported for this commercial alloy. The material processed during run 2, denoted as FSP (Ex2) in figure 8, has a grain size